Geometry of Taylor Bubbles Rising through Liquid-Filled Annuli

G. Das, N. K. Purohit and A. K. Mitra
Dept. of Chemical Engineering, Indian Institute of Technology, Kharagpur 721302, India

P. K. Das
Dept. of Mechanical Engineering, Indian Institute of Technology, Kharagpur 721302, India

During the co-current flow of gas and liquid through any conduit, one of the commonly encountered flow regimes is slug flow. This flow pattern is characterized by the alternate succession of Taylor bubbles and liquid slugs. The pressure drop and the rates of the different transport processes in slug flow depend tremendously on the characteristics of these elongated bubbles. This has motivated numerous studies in circular tubes to understand their behavior. A Taylor bubble in a circular tube is axisymmetric and is characterized by a blunt bullet-shaped nose and a cylindrical tail. This typical shape influences their velocity of upward movement through liquid. Considering potential flow past the bubble nose, the rise velocity of such bubbles has been derived by Dumitrescu (1943) and Davis and Taylor (1950). Their shape has also been found out experimentally either by photographic techniques (Davis and Taylor, 1950; Brown, 1965) or by conductivity probes measurements (Mao and Dukler, 1991).

On the other hand, not much information is available regarding the geometry and other characteristics of Taylor bubbles through concentric annuli. Some efforts (Griffith, 1964; Sadatomi et al., 1982; Caetano et al., 1989; Hills and Chetty, 1998) have been made to determine experimentally their rise velocity through liquid-filled annuli. Most of these investigations have reported an asymmetric shape of the bubble wrapping only partially of the inner tube of the annulus. However, these studies neither provide any explanation for this asymmetric shape, nor could they relate the rise velocity to the bubble geometry. Kelessidis and Dukler (1990) showed that the Taylor bubbles should have an asymmetric shape in an annulus to rise at the maximum velocity. They idealized the bubble in an annular passage as a two-dimensional (2-D) bubble of uniform thickness and determined the rise velocity assuming potential flow past it. The analysis of Kelessidis and Dukler (1990) was later modified by Das et al. (1998). They have considered the 3-D shape of the bubbles and accounted for the film thickness, while deriving the rise velocity as a function of the annulus dimensions. The predictions of Das et al. (1998) showed a better agreement with their own experiments, as well as with the results published in literature. Nevertheless, to the best of the authors' knowledge, no experimental investigations have so far been reported for determining the complete geometry of Taylor bubbles in an annulus.

Figure 1 shows the shape of the Taylor bubble in an annulus as described in literature *vis-à-vis* that in a circular tube. The figure shows that the Taylor bubble in a concentric annulus does possess a nose of a variable cross-section and a constant area tail very similar to its counterpart in a circular tube. However, it is not axisymmetric and has an elliptic nose. While the radius of curvature of the nose and of the liquid film thickness around the tail completely characterizes a Taylor bubble in a circular tube, the important dimensions of the bubble in the latter geometry include the semi-major and minor axes of the elliptic nose, the angle of wrap, and the thickness of the two liquid films between the bubble and the inner and outer walls of the conduit. Therefore, the methods used so far for the measurement of bubble shape in a circular tube cannot be applied directly in an annulus.

In the present work, an altogether different approach has been devised for determining the bubble geometry. The conductivity probe measurement has been used to find out the length-volume relationship of Taylor bubbles rising through liquid-filled annuli. This information has been used along with an approximate mass balance equation to determine the important geometric parameters of the Taylor bubble. Finally, the analysis of Das et al. (1998) has been extended to determine (purely on a theoretical basis) the bubble geometry, and a comparison has been made.

Correspondence concerning this article should be addressed to P. K. Das.

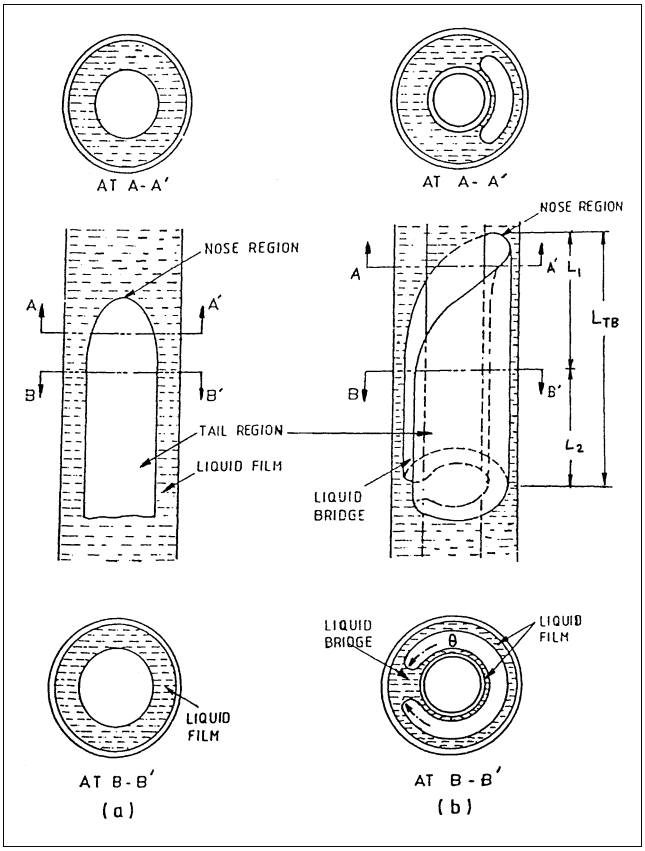

Figure 1. Taylor bubble rising through: (a) circular tube; (b) concentric annulus.

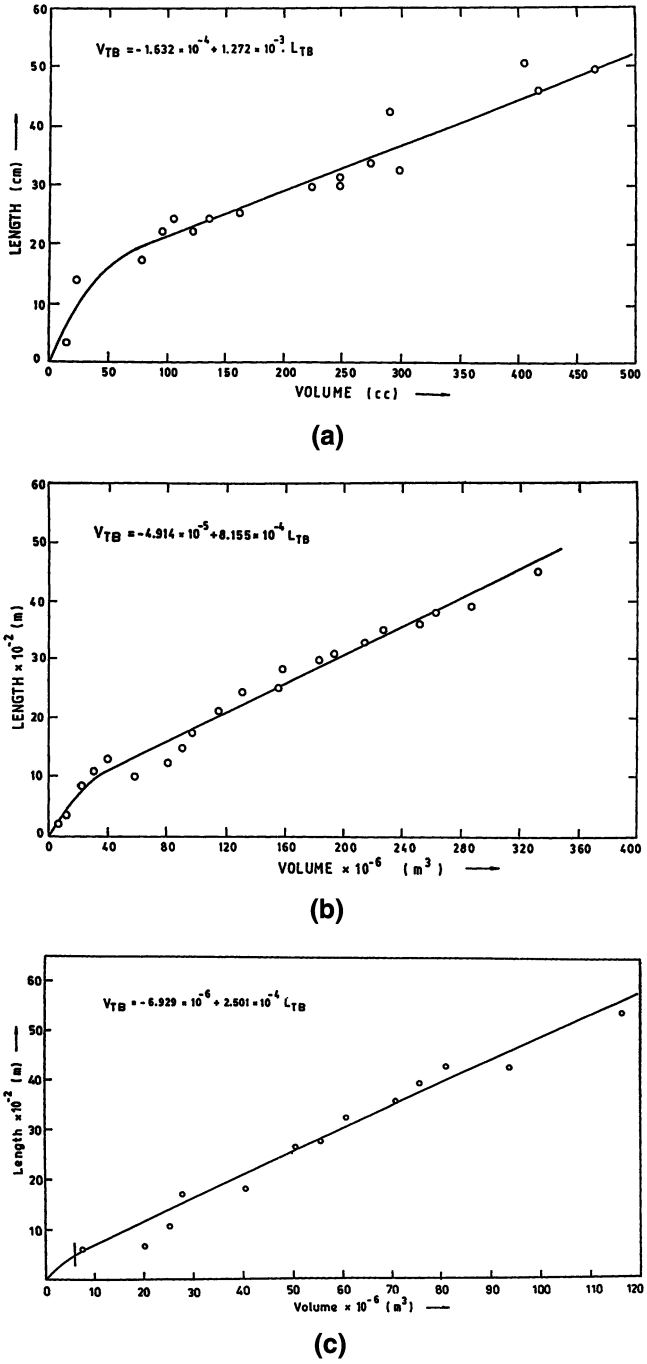

Figure 2. Experimental curves of length vs. volume for: (a) Annulus A; (b) Annulus B; (c) Annulus C.

Experimental Studies

The details of the test facility have been described in Das et al. (1998). Experiments have been performed in three different annular test sections: A, B, and C with O.D. of 0.0508 m, 0.0381 m, and 0.0254 m and I.D. of 0.0254 m, 0.0127 m, and 0.0127 m, respectively. The setup facilitates the generation of Taylor bubbles of predetermined volume. Parallel plate type conductivity probes of a unique design have been employed for the measurement of bubble lengths and of rise velocities. The passages of the bubble across a probe is noted by a peak in the output signal. A pair of the probes located at a known distance apart has been used to determine the rise velocity. For a known rise velocity, the bubble lengths have been determined from the peaks of the individual signals. The experiments have been performed for a wide range of bubble volumes which have been selected so that the length of the entrapped air in the circular entry section ranges from 0.5 to 20 times the hydraulic diameter of the annulus.

Analysis of Experimental Results

The length–volume relationship as obtained experimentally for bubbles of different dimensions in the three annuli is shown in Figures 2a, 2b, and 2c. The figures show that for a small volume, the bubble length can be correlated with the corresponding volume by a curved line from the origin. This continues until a critical bubble volume is reached. Beyond this, the relationship between length and volume becomes linear. The equations of the straight lines are

$$V_{TB} = -1.632 \times 10^{-4} + 1.272 \times 10^{-3} L_{TB} \quad (1)$$

$$V_{TB} = -4.914 \times 10^{-5} + 8.155 \times 10^{-4} L_{TB} \quad (2)$$

$$V_{TB} = -6.929 \times 10^{-6} + 2.501 \times 10^{-4} L_{TB} \quad (3)$$

for annuli A, B and C, respectively, where L_{TB} is the total length of a fully formed Taylor bubble of volume V_{TB}.

The nature of the curves indicates that for bubble volumes less than the nose volume, the cross-sectional area increases with length. Once the nose is formed, the excess volume of air merely increases the length of the tail region without altering its shape. Thus, the length and volume of the nose region is obtained from the intersection of the nonlinear and linear portions of the curves in the three figures. The unique intersection point shows that the nose of a fully formed Taylor bubble is independent of bubble volume and a function of annulus dimensions only.

The tail dimensions are estimated by comparing Eqs. 1, 2 and 3 with the expression of bubble volume as a summation of its nose volume V_1 and tail volume, A_2L_2

$$V_{TB} = V_1 + A_2L_2 \tag{4}$$

Or,

$$V_{TB} = (V_1 - A_2L_1) + A_2L_{TB} \tag{5}$$

Note that in Figure 1b, L_1 is the length of the nose region where the cross-sectional area of the bubble increases from the tip until it attains a constant value, and L_2 that of the tail region where the cross-sectional area remains unchanged.

Equation 5 is in a form equivalent to that of Eqs. 1, 2 or 3, and a comparison between the different terms of these equations brings out certain interesting features. First, as the cross-sectional area of the tail region is higher than that of the nose region, V_1 is less than A_2L_1. This is brought out by the negative intercepts of Eqs. 1–3. Secondly, the coefficient of L_{TB} in Eqs. 1–3 is a direct measure of the cross-sectional area A_2 occupied by the tail region in the three annuli.

In order to evaluate the remaining parameters of the bubble, area A_2 has been expressed geometrically referring to Figure 3, which represents the symmetric half of the bubble cross-section.

$$A_2 = 2\,(\text{Area } ABCD + \text{Area } CED)$$

$$= \left[(r_2 - \delta_2)^2 - (r_1 + \delta_1)^2\right][\theta - \theta'] + \frac{\pi}{4}[r_2 - r_1 - \delta_2 - \delta_1]^2 \tag{6}$$

Subsituting θ' in terms of other geometry parameters, A_2 can be written as

$$A_2 = \left[(r_2 - \delta_2)^2 - (r_1 + \delta_1)^2\right]\left[\theta - \frac{r_2 - r_1 - \delta_2 - \delta_1}{r_1 + r_2}\right] + \frac{\pi}{4}[r_2 - r_1 - \delta_2 - \delta_1]^2 \tag{7}$$

Where r_1 and r_2 are the inner and outer radii of the annulus, δ_1 and δ_2 are the respective thickness of the liquid films at the two walls, θ is the angle of wrap, and θ' is the angle subtended by the round edge of the bubble, as shown in Figure 3.

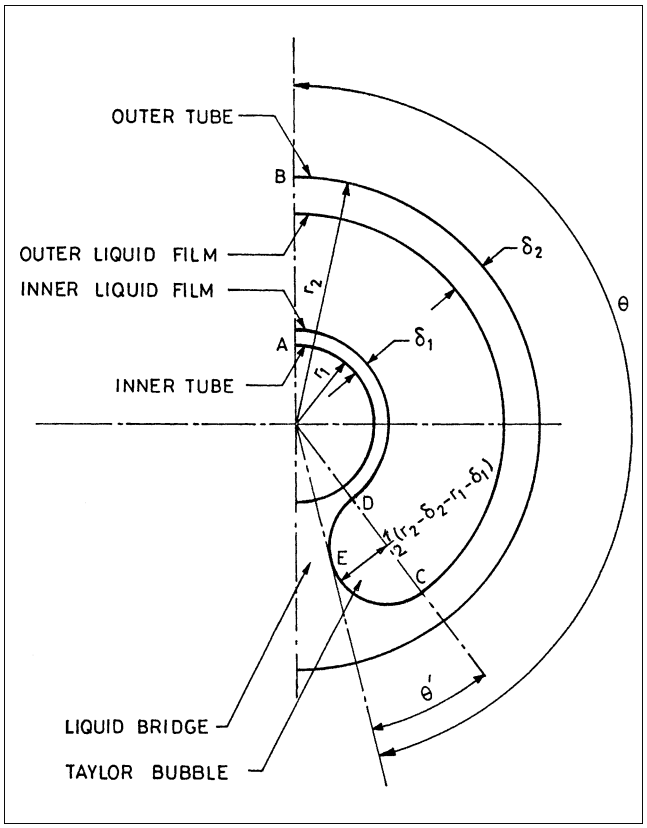

Figure 3. Cross-sectional view of a symmetric half of a Taylor bubble in a concentric annulus.

A force balance for the liquid films over the two walls of the annulus and the constant pressure condition inside the bubble implies equal thickness δ of the two films. This gives the expression of A_2 as

$$A_2 = \left[(r_2 + r_1)(r_2 - r_1 - 2\delta)\right]\left[\theta - \frac{r_2 - r_1 - 2\delta}{r_1 + r_2}\right] + \frac{\pi}{4}[r_2 - r_1 - 2\delta]^2 \tag{8}$$

The closure equation for evaluating the individual values of the two unknown parameters δ and θ has been obtained from a mass balance of liquid flow between a plane far upstream from the bubble and at the intersection between the nose and the tail region (BB' in Figure 1). Assuming a vertically downward flow of liquid, the equation is

$$\frac{1}{3}\frac{g\delta^3}{\gamma}(r_1 + r_2)\theta = A_2U \tag{9}$$

where U is the rise velocity of a Taylor bubble in liquid-filled annular columns, g is the acceleration due to gravity, and γ is the kinematic viscosity of the liquid.

The geometric parameters of Taylor bubbles thus obtained for the three annuli are listed in Table 1.

Table 1. Bubble Geometry from Experiments

Annulus No.	$L_1 \times 10^{-2}$ (m)	$V_1 \times 10^{-5}$ (m^3)	θ (rad)	$\delta \times 10^{-4}$ (m)
A	9.21	7.0	4.73	7.325
B	6.35	3.15	4.322	6.89
C	5.0	7.8	3.88	4.83

Theoretical Analysis

A theoretical relationship between the length and volume of Taylor bubbles is obtained by evaluating the nose and tail volumes in Eq. 4. Although Kelessidis and Dukler (1990) had assumed the Taylor bubble as a 2-D bubble of constant thickness, in reality a curvature does exist over the edge of the Taylor bubble from its nose to tail.

If a Taylor bubble is unwrapped and laid on a flat surface, it can be represented by Figure 4. The part of the bubble shown by firm lines is half of an ellipse with a and b as its semi-major and semi-minor axis, respectively. There is a curved edge whose cross-sectional area is a semi-circle wrapped over the semi-ellipse. This appears like a crown over the bubble nose and is represented by a dotted line in Figure 4. Accordingly, the nose volume V_1 is the summation of the volume of the 2-D nose V_1' and the volume of the curved edge V_{crown}

$$V_1 = V_1' + V_{\text{crown}} \tag{10}$$

V_1' may be obtained by multiplying the thickness of the bubble with the area of the semi-ellipse ($\pi ab/2$). The cross-sectional area of the crown [$\pi/8\ (r_2 - r_1 - 2\delta)^2$] when multiplied with the perimeter of the semi-ellipse gives V_{crown}. The perimeter of an ellipse is a function of its axes and can be represented by an infinite series. In order to obtain a closed form expression without a significant loss of accuracy, the perimeter has been approximated as $\pi(a+b)$. This gives V_1 as

$$V_1 = \frac{\pi ab}{2}\ (r_2 - r_1 - 2\delta) + \frac{\pi^2}{16}(r_2 - r_1 - 2\delta)^2(a+b) \tag{11}$$

The volume V_2 (A_2L_2) of the tail region can be obtained using the expression of A_2 given in Eq. 8. Substitution of Eqs. 8 and 11 in Eq. 5 gives the volume of a fully formed Taylor bubble V_{TB} as

$$V_{TB} = p + qL_{TB} \tag{12}$$

where

$$p = \frac{\pi ab}{2}(r_2 - r_1 - 2\delta) + \frac{\pi^2}{16}(r_2 - r_1 - 2\delta)^2(a+b) - (r_2 + r_1)(r_2 - r_1 - 2\delta)\left(\theta - \frac{r_2 - r_1 - 2\delta}{r_2 + r_1}\right)\left(a + \frac{r_2 - r_1 - 2\delta}{2}\right) - \frac{\pi}{4}(r_2 - r_1 - 2\delta)^2\left(a + \frac{r_2 - r_1 - 2\delta}{2}\right) \tag{13}$$

$$q = (r_2 + r_1)(r_2 - r_1 - 2\delta)\left[\theta - \frac{r_2 - r_1 - 2\delta}{r_2 + r_1}\right] + \frac{\pi}{4}(r_2 - r_1 - 2\delta)^2 \tag{14}$$

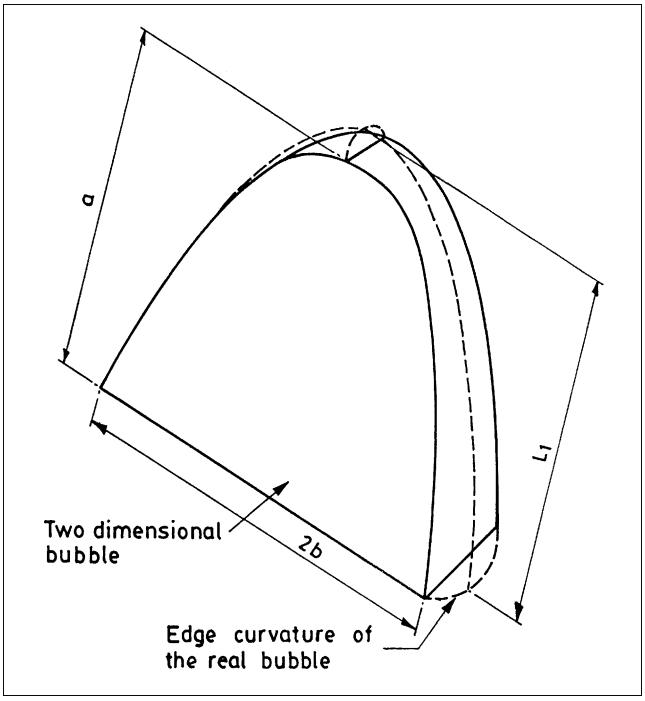

Figure 4. 2-D elliptic bubble and its corresponding real bubble.

The geometric parameters required to determine the theoretical relationship between length and volume includes the semi-major and minor axes of the elliptic cap, as well as the angle of wrap and the liquid film thickness in the tail region. They have been estimated from a modified potential flow analysis, which considers inviscid flow at the nose and incorporates the effect of viscosity in the liquid films at the tail region. The model yields rise velocity and bubble geometry from annulus dimensions as its input parameters. The details of the analysis has been presented in Das et al. (1998). The geometric parameters obtained from the model are listed in Table 2 and used in Eq. 12. The equation shows that the theoretical analysis has also yielded the linear relationship between length and volume of fully formed Taylor bubbles in

Table 2. Bubble Geometry from Theory

Annulus No.	$L_1 \times 10^{-2}$ (m)	$V_1 \times 10^{-5}$ (m^3)	2θ (rad)	$\delta \times 10^{-4}$ (m)
A	9.51	7.044	4.79	7.25
B	6.48	3.36	4.613	6.79
C	6.8	8.92	3.648	5.02

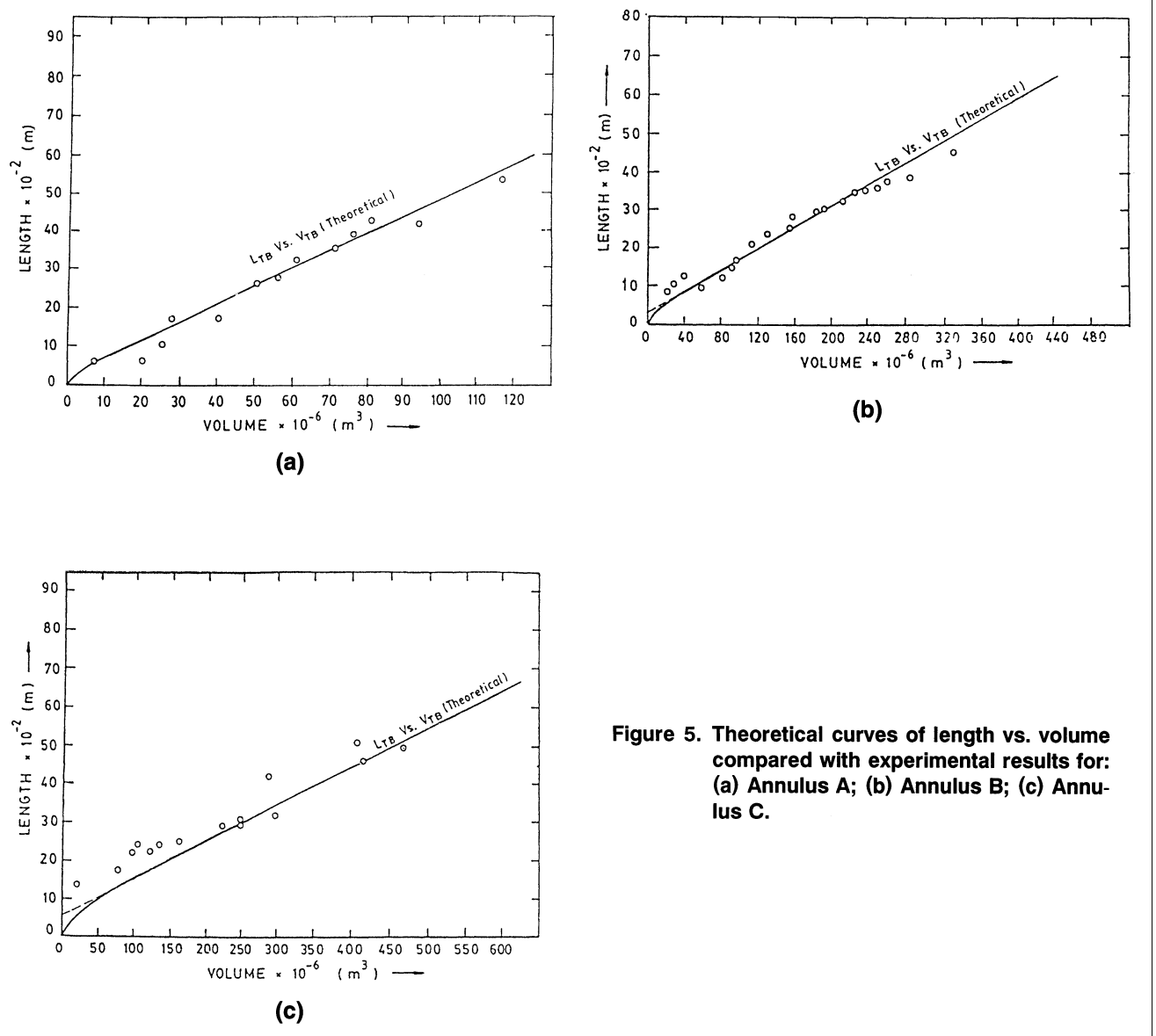

Figure 5. Theoretical curves of length vs. volume compared with experimental results for: (a) Annulus A; (b) Annulus B; (c) Annulus C.

agreement with the experimental results. Moreover, both the theory and the experiments show that the geometry of a Taylor bubble rising through liquid-filled concentric annulus is a function of the annulus dimensions.

The data in Table 2 agree well with those reported in Table 1. Further, a comparison of Eq. 12 as shown in Figures 5a, 5b, and 5c for the three annuli with the experimental data plotted in the corresponding figures also proves the validity of the models.

Conclusions

This article attempts to predict the geometry of Taylor bubbles rising through concentric annulus both from experiments, as well as theoretical analysis. The experimentally determined length–volume relationship along with a mass conservation equation have been used to estimate the important parameters necessary for describing a Taylor bubble in this doubly connected flow passage. Both experiment and theory have yielded a linear relationship between the lengths and volumes of fully formed bubbles. The experimental results have also shown that the nose and the angle of the wrap of these bubbles are independent of bubble volume and a function of annulus dimensions only. Once the nose is formed, the excess volume of air merely increases the length of the Taylor bubbles without affecting their shape in agreement to the observations reported for circular tubes. The satisfactory agreement between experiment and theory takes note that the analysis proposed by Das et al. (1998) can be used to predict the geometry of Taylor bubbles rising through concentric annuli without any experimental parameter as its input.

Literature Cited

Brown, R. A. S., "The Mechanics of Large Bubbles in Tubes: I. Bubble Velocities in Stagnant Liquids," *Canadian J. of Chem. Eng.*, 217 (Oct. 1965).

Caetano, E. F., O. Shoham, and J. P. Brill, "Upward Vertical Two Phase Flow through an Annulus-Part I. Single Phase Friction Factor, Taylor Bubble Rise Velocity and Flow Pattern Prediction," *Multiphase Flow Proc. Int. Conf.*, BHRA, Cranfield, England, 301 (1989).

Das, G., P. K. Das, N. K. Purohit and A. K. Mitra, "Rise of Taylor Bubbles through Concentric Annuli," *Chem. Eng. Sci.*, **53**, 977 (1998).

Davies, R. M., and G. Taylor, "The Mechanics of Large Bubbles Rising through Extended Liquids and Through Liquids in Tubes," *Proc. Roy. Soc. Ser.*, 200A, 375 (1950).

Dumitrescu, D. T., "Stromung an Einer Lufblase im Senkrechten Rohr," *SAMM*, **21**, 139 (1943).

Griffith, P., "The Prediction of Low Quality Voids," *J. Heat Trans. ASME*, **86C**, 327 (1964).

Hills, J. H., and P. Chety, "The Rising Velocity of Taylor Bubbles in an Annulus," *Trans. I. Chem E.*, **76**, Part A, 723 (Sept. 1998).

Kelessidis, V. C., and A. E. Dukler, "Motion of Large Gas Bubbles through Liquids in Vertical Concentric and Eccentric Annuli," *Int. J. Multiphase Flow*, **16**, 375 (1990).

Mao, Zai-Sha, and A. E. Dukler, "The Motion of Taylor Bubbles in Vertical Tubes: II. Experimental Data and Simulations for Laminar and Turbulent Flow," *Chem. Eng. Sci.*, **46**, 2055 (1991).

Sadatomi, M., Y. Sato, and S. Saruwatari, "Two Phase Flow in Vertical Non-Circular Channels," *Int. J. Multiphase Flow*, **8**, 641 (1982).

Manuscript received June 12, 2000, revision received June 4, 2001.